Journal of Materials Chemistry C

PAPER

Cite this: J. Mater. Chem. C, 2015, 3, 601

Polycyclic anthanthrene small molecules: semiconductors for organic field-effect transistors and solar cells applications†

Jean-Benoît Giguère,[a] Niyazi Serdar Sariciftci[b] and Jean-François Morin*[a]

Received 22nd September 2014
Accepted 10th November 2014

DOI: 10.1039/c4tc02137a

www.rsc.org/MaterialsC

Anthanthrene small molecules with different pendant groups were investigated as semiconductors for organic field-effect transistors and solar cells. Field-effect mobilities were greatly improved with solvent annealing and reached maximum values of 0.078 $cm^2\ V^{-1}\ s^{-1}$ for a thiophene-appended anthanthrene derivative. When used as donors in conjunction with $PC_{61}BM$ in bulk heterojunction solar cells, a maximum PCE of 2.4% was achieved with good V_{OC} and FF of 0.77 V and 59%, respectively. Although solvent annealing induced J-aggregation of all anthanthrene compounds, such processing step did not necessarily improved the solar cell *J–V* characteristics as opposed to the field effect mobility. The results showcase the potential of the polycyclic anthanthrene core as a building block for organic electronics.

Introduction

Polycyclic aromatic compounds are becoming increasingly popular as alternatives to linearly fused acene compounds for optoelectronic applications.[1–8] From a charge transport standpoint, their extended π-conjugation, both in length and "area", could be beneficial since intermolecular overlap (electronic coupling) increases with respect to size. Besides, reorganization energies should be kept low because of their intrinsic structural rigidity.[1,8,9] The optoelectronic properties of such polycyclic systems are highly dependent on how aromatic rings are fused together: this determines the type of edges (zigzag *versus* armchair) and the number of benzenoid Clar's aromatic sextets, which govern the aromatic stabilization energy, such as stated by Clar's rules.[10] Complex synthetic routes and solubility hurdles of such large polycyclic can become a limiting factor and might have hindered their widespread adoption as materials of choice.[1] In a recent report, Briseno *et al.*[9] synthesized bistetracene compounds, which afforded an impressive combination of field-effect mobility over 6 $cm^2\ V^{-1}\ s^{-1}$ and good ambient stability. This showcases the high potential of annulated acene compounds for organic field-effect transistors (OFET) and solar cells (OSC), notably because of their highly tunable properties such as broad absorption and tailorable molecular packing.[11–13] For instance, we have previously shown for the anthanthrene scaffold that the conjugation can be effectively extended through the 6,12-positions whereas the 4,10-positions had a very limited impact on the opto-electronic properties.[14] Although a few anthanthrene derivatives has been reported by us and others,[14–19] very few compounds have actually been investigated in organic electronic devices. An exception is the 6,12-triisopropylsilylethynylanthanthrene employed as a donor in solar with an efficiency of about 2%.[20] Good charge-transport properties have been determined computationally but very limited hole mobility in the order of 10^{-5} $cm^2\ V^{-1}\ s^{-1}$ were measured in OFET.[21] Also, a recent review covers the current status of alkyne containing small molecule semiconductors for organic electronic.[22] We decided to investigate compound **1–3**[14] in order to assess the potential of anthanthrene small molecules as semiconductor for OPV and OFET because of their ease of preparation from a cost-efficient, commercially available VAT dye, good stability and solubility. Compounds **1–3** (Fig. 1) are structurally similar with the same hexacyclic aromatic fused core and are decorated with

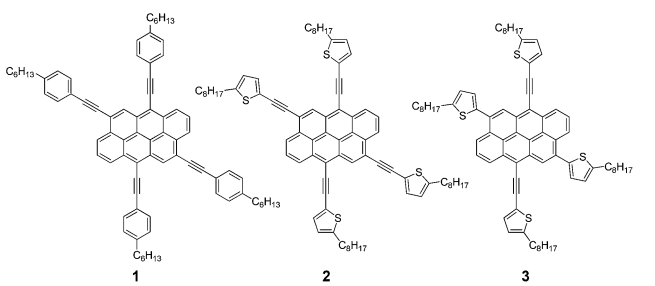

Fig. 1 Structure of cruciform anthanthrene compound **1**, **2** and **3**.

[a]*Département de Chimie et Centre de Recherche sur les Matériaux Avancés (CERMA), Université Laval, Pavillon A.-Vachon, 1045 Ave de la Médecine, Québec, G1V 0A6, Canada. E-mail: jean-francois.morin@chm.ulaval.ca; Fax: +1-418-656-7916; Tel: +1-418-656-2812*

[b]*Linz Institute for Organic Solar Cells (LIOS), Johannes Kepler University Linz, Altenbergerstrasse 69, 4040 Linz, Austria*

† Electronic supplementary information (ESI) available: Output characteristics and supplementary EQE, UV-vis spectra and AFM images. See DOI: 10.1039/c4tc02137a

4-hexylbenzene and 5-octylthienyl groups at the 4,6,10,12-positions either directly or with an acetylenic linker in order to reduce the torsion angle between the two aromatic units.

Results and discussion

Organic field-effect transistors

In order to assess the mobility of the anthanthrene polycyclic scaffold in OFETs, a bottom-gate bottom-contact (BCBG) device configuration (Fig. 2) with Si/SiO_2 substrate was used because of its ease of fabrication, robustness and high device reproducibility. An octadecyltrimethoxysilane (ODTS) self-assembled monolayer (SAM) was used as dielectric surface modifier in order to improve the hydrophobicity and the semiconductor–dielectric interface.[23] The semiconductors were spin-coated from chloroform solutions at a concentration of 10 mg ml^{-1}. It should be noted that uniform films could not be obtained from higher boiling point solvents such as toluene or chlorobenzene because of dewetting during spin-coating, a common problem for small molecules semiconductors.[24,25]

The hole charge carrier mobility measured on the as-cast films of compounds **1–3** were at most 10^{-3} cm^2 V^{-1} s^{-1}, see Table 1. The poor organization (*vide infra*) in the as-cast film was surprising considering that these compounds have a strong tendency to aggregate in solution[14] and that analogous cruciform compounds based on the anthracene scaffold provided excellent mobilities without any post-processing.[26,27] The fast drying time of low boiling point chloroform at high spin rates (5000 rpm) certainly limits the self-organization and crystalline growth. Although thermal annealing is the most commonly used annealing process, the performance gain proved limited in our case (unreported preliminary results), which is corroborated by a thin film UV-vis absorption study of **1** with different treatment (Fig. 3). Thermal annealing at 80 °C had no effect on the absorbance spectrum whereas solvent annealing with toluene (covered Petri dish, 1 hour) lead to a significant increase of the lower energy absorption band, which is generally assigned to J-aggregation.[28] Solvent annealing with a good (toluene) and a marginal (cyclohexane) solvent lead to a significant increase in the charge mobility (30-fold increase) for **1** with cyclohexane, leading to a maximum mobility of 0.015 cm^2 V^{-1} s^{-1}. All anthanthrene derivatives behaved similarly with a gain of at least an order of magnitude in mobility using a simple solvent annealing step. Although shorter annealing time (<15 minutes) lead to improved characteristics, a longer

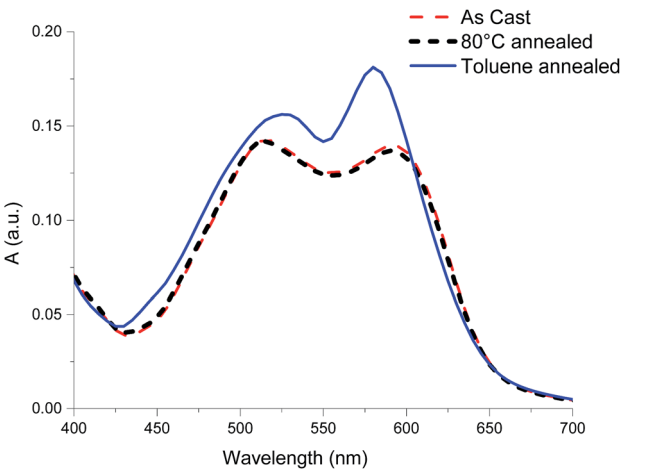

Fig. 3 UV-vis film absorption of compound **1** with different annealing conditions.

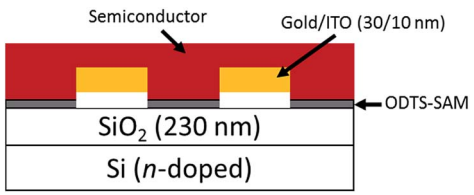

Fig. 2 Bottom-gate bottom-contact transistor stack.

Table 1 Transistor characteristics for compounds **1**, **2** and **3**

Compound	μ_{sat}[a] (cm^2 V^{-1} s^{-1})	V_{th} (V)	$I_{on/off}$	Annealing
1	4.3 (5.2) × 10^{-4}	5	10^4	As cast
	8.9 (10) × 10^{-3}	4	10^5	Toluene
	1.3 (1.5) × 10^{-2}	**3**	$\mathbf{10^5}$	**Cyclohexane**
2	1.0 (1.5) × 10^{-4}	9	—	As cast
	2.0 (2.3) × 10^{-3}	**19**	$\mathbf{10^3}$	**Toluene**
	1.4 (1.7) × 10^{-3}	19	10^3	Cyclohexane
3	6.4 (6.7) × 10^{-3}	−9	10^5	As cast
	6.5 (7.8) × 10^{-2}	**−6**	$\mathbf{10^6}$	**Toluene**
	3.4 (4.9) × 10^{-2}	−6	10^6	Cyclohexane

[a] Average hole mobility measured in the saturation regime measured over 4 devices. Maximum mobility are reported in parenthesis.

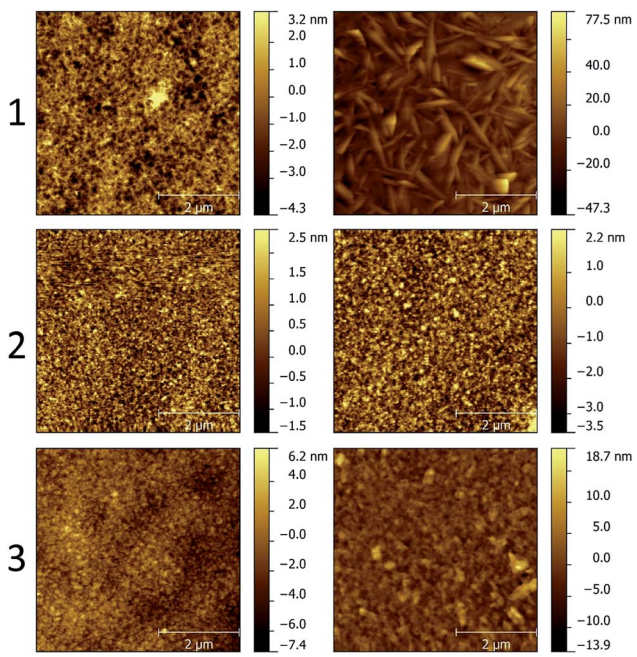

Fig. 4 AFM height topography of thin film of **1–3** (top, middle, bottom respectively) before (left) and after (right) toluene annealing.

treatment of one hour proved optimal. The transfer curves under the optimal conditions are reported in Fig. 5 and the output curves in Fig. S1–S3.† Compound **3** treated with toluene vapor afforded the best performance with a maximum mobility of 0.078 $cm^2\ V^{-1}\ s^{-1}$, an on/off ratio of over 10^6 and a low threshold voltage of −6 V.

The topography of the thin films were analyzed using AFM and compounds **1–3** produced smooth as-cast films whereas toluene annealing only induced a clear crystallization for compound **1** with the formation of hundreds of nanometers long needle-like crystallites (Fig. 4). For compounds **2** and **3** a small increase in roughness was observed but no long range features. Large plate-like single crystals of **3** were grown from solution but unfortunately we were unable to solve its structure

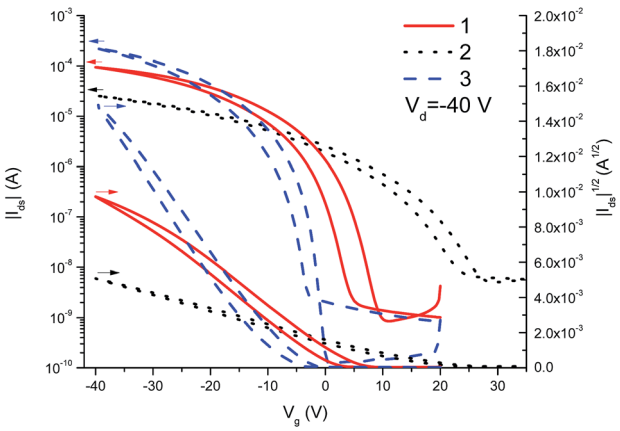

Fig. 5 Transfer characteristics after cyclohexane solvent annealing for compound **1** and toluene annealing for compound **2** and **3**.

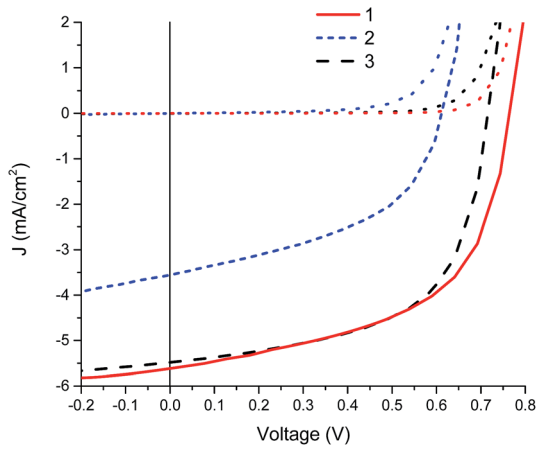

Fig. 6 *J–V* curves for compounds **1** (as cast), **2** (80 °C annealed) and **3** (toluene annealed) at a D/A ratio of 1 : 0.7 under illumination and dark (short dotted lines) under the optimized conditions reported in bold in.

because of defects. Without a crystal structure, it is difficult to perform a structure–property analysis but it seems reasonable to speculate that the four peripheral solubilizing alkyl chains at the 4,6,10 and 12 positions limit the interstack transfer integral.[8] A simple solution to improve the charge transport properties would be to get rid of the pendant groups in either the 4,10 or the 6,12 axes to shorten the interstack distances and facilitate charge transfer.

Bulk heterojunction solar cells

The HOMO levels of compounds **1–3** (as determined by cyclic voltammetry) are 5.35, 5.31 and 5.23 eV, respectively, with an

Table 2 Bulk heterojunction solar cell parameters[a]

Donor compound	D/A (wt ratio)	Annealing	V_{OC} (V)	J_{SC} (mA cm^{-2})	FF (%)	PCE[c] (%)	R_s (Ω)	R_p (kΩ)	d^d (nm)
1	**1 : 0.7**	—	**0.77**	**5.3**	**55**	**2.2 ± 0.1 (2.4)**	**107**	**32**	**77**
	1 : 0.7	80 °C	0.71	4.9	59	2.0 ± 0.1 (2.2)	47	14	77
	1 : 0.7	Toluene	0.77	3.1[b]	39	1.0 ± 0.1 (1.1)	321	24	77
	1 : 1	—	0.76	5.3	52	2.1 ± 0.2 (2.4)	81	18	87
	1 : 1	80 °C	0.71	4.7	59	2.0 ± 0.1 (2.1)	49	16	87
	1 : 2	—	0.75	2.6	46	1.0 ± 0.1 (1.1)	161	22	130
	1 : 2	80 °C	0.68	2.3	55	0.9 ± 0.0 (0.9)	81	30	130
2	1 : 0.7	—	0.61	3.1	47	0.9 ± 0.1 (1.0)	31	6.6	80
	1 : 0.7	**80 °C**	**0.59**	**3.5**	**47**	**1.0 ± 0.1 (1.07)**	**26**	**7.8**	**80**
	1 : 0.7	Toluene	0.55	3.5[b]	44	0.9 ± 0.1 (0.9)	24	1.8	80
3	1 : 0.5	—	0.73	4.6	46	1.5 ± 0.1 (1.6)	90	8.7	75
	1 : 0.5	80 °C	0.70	3.9	51	1.4 ± 0.1 (1.5)	81	8.3	75
	1 : 0.5	Toluene	0.75	4.6	56	1.9 ± 0.2 (2.3)	152	13	75
	1 : 0.7	—	0.68	4.0	39	1.1 ± 0.1 (1.2)	100	1.8	83
	1 : 0.7	80 °C	0.70	4.7	49	1.6 ± 0.1 (1.7)	73	9.4	83
	1 : 0.7	**Toluene**	**0.74**	**4.9**	**59**	**2.1 ± 0.1 (2.3)**	**77**	**14**	**83**
	1 : 1	—	0.69	2.7	38	0.7 ± 0.1 (0.8)	106	5.2	87
	1 : 1	80 °C	0.68	3.4	47	1.1 ± 0.1 (1.1)	64	7.8	87
	1 : 1	Toluene	0.74	4.6	57	1.9 ± 0.1 (2.0)	64	13	87
	1 : 2	Toluene	0.72	3.2	47	1.1 ± 0.1 (1.2)	57	10	110

[a] Average data of at least 6 cells measured under 100 mW cm^{-2} AM 1.5G illumination. [b] Measured at 80 mW cm^{-2} illumination with J_{sc} normalized to 100 mW cm^{-2} for clarity. [c] Maximum efficiency presented in parentheses. [d] Thickness of the active layer.

equal optical bandgap of 1.9 eV.[14] Therefore, they are suitable donors for organic solar cells with [6,6]-phenyl-C61-butyric acid methyl ester ($PC_{61}BM$) fullerene acceptor.[29] A bulk heterojunction solar cell configuration with ITO/PEDOT:PSS/Donor:PC_{61}BM/LiF/Al was used to optimize the active layers. The active layers were spin-coated from $CHCl_3$ solutions with a donor concentration of 10 mg ml^{-1} with different weight ratios of PCBM. The summarized results are reported in Table 2 with the optimal processing conditions in bold along with the *J–V* curves in Fig. 6. Donor **3** was investigated first to determine the effect of the donor/acceptor (D/A) ratio and the different processing parameters on the photovoltaic performance because of its higher field-effect mobility. For compound **3**, under all D/A ratios investigated (from 1 : 0.5 to 1 : 2), solvent annealing proved to be a superior treatment than thermal annealing and improved all of the *J–V* characteristics. The effect of the annealing conditions at the optimal D/A ratio of 1 : 0.7 on the external quantum efficiency (EQE) is presented in Fig. 7. At the absorption maxima, the EQE stays fairly constant at around 40% but is shifted to lower energy after annealing, attributed to the formation of J-aggregates, which interestingly leads to an increase of 0.06 eV in V_{oc}.

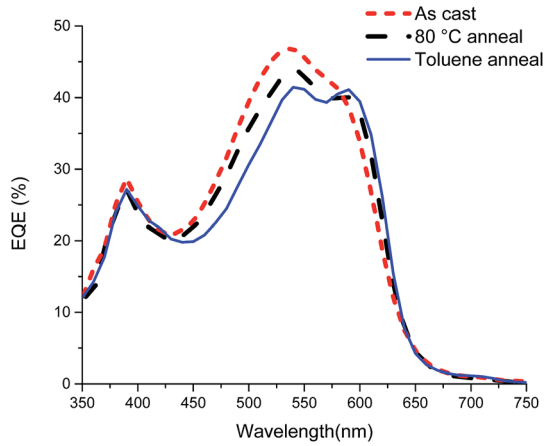

Fig. 7 EQE for **3** : $PC_{61}BM$ at a ratio of 1 : 0.7 with different treatments.

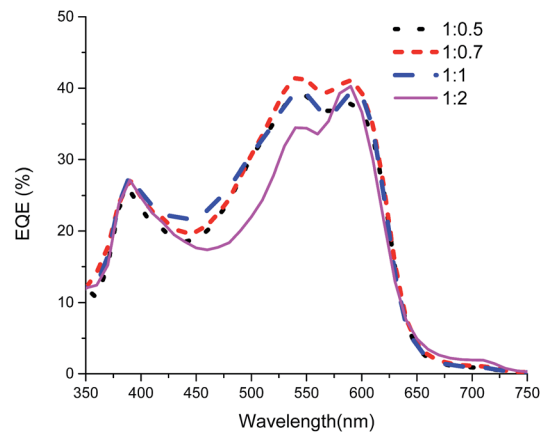

Fig. 8 EQE for **3** : $PC_{61}BM$ at different D/A ratios after toluene annealing.

The J_{sc} and FF are also increased to 4.9 mA cm^{-2} and 59%, respectively. The PCE and EQE (Fig. 8) is weakly dependent on the D/A ratio from 1 : 0.5 to 1 : 2, decreasing with increasing $PC_{61}BM$ content, probably because of the thicker layer leading to diminished charge extraction. It appears that under the actual conditions, the current density is the limiting factor to a high efficiency device and the weak dependence of the EQE on the PCBM content is indicative of suboptimal active-layer morphologies whereas the high fill factor supports a balanced electron and hole mobility.[30] Interestingly, the presence of $PC_{61}BM$ even at high concentration does not limit the formation of the J-aggregates as the measured EQE (Fig. 8) is higher at longer wavelength and is in accordance with the UV-vis data (Fig. S4†). For compound **1**, annealing lead to a deterioration of the *J–V* characteristics as can be expected by the formation of large crystallites (Fig. 4) whereas it had a limited effect on compound **2**. This in contrast to compound **3** as the field-effect mobilities for all compounds were greatly improved with solvent annealing.

For the optimal mixture of **1** : $PC_{61}BM$ (1 : 0.7), the device characteristic from the as cast film are the best obtained for these anthanthrene small molecules with a maximum PCE of 2.4%. Although toluene annealing induced J-aggregation at all PCBM concentrations for compound **1** (Fig. 9 and S6† for EQE), the *J–V* characteristics are worsened with a significant drop in J_{sc} and FF. Compound **2** was tested solely at a D/A ratio of 1 : 0.7,

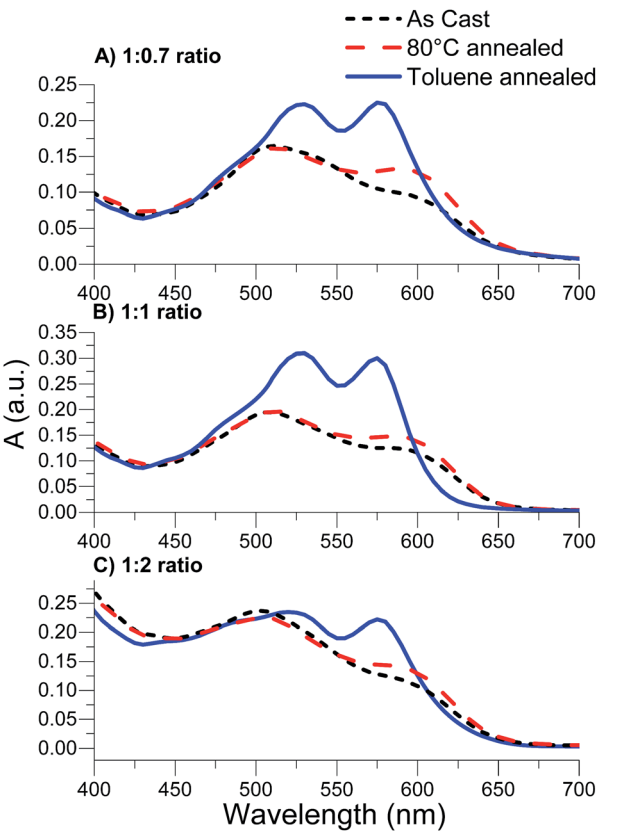

Fig. 9 UV-vis film absorption of compound **1** at different ratio of $PC_{61}BM$ with different annealing conditions.

which resulted in a lower PCE of 1.0% after thermal annealing with a V_{oc} 0.15 V lower than **1**. Because of its lower field-effect mobility and V_{oc}, we did not investigate this compound further. Interestingly, although the field-effect mobility of **2** is the lowest among the tested molecules, it achieved the solar cells with the lowest series resistance (R_s), comparable to a P3HT standard device under the same device structure. The devices prepared with compounds **1** and **3** had higher series resistance, which is certainly a factor limiting the overall device efficiency.[20]

Conclusions

In summary, we have investigated anthanthrene compounds as p-type semiconductors in OFETs and OSCs. Solvent annealing proved to be necessary to induce J-aggregation and achieve good field-effect mobilities reaching a maximum of 0.078 $cm^2 V^{-1} s^{-1}$ for compound **3**. When used as donors with $PC_{61}BM$ in a standard BHJ, solvent annealing induced J-aggregation at all D/A ratios but a significant improvement of the power conversion efficiency was only observed for **3**. Although the as cast film of compound **1** lead to a poor field-effect mobility they afforded an optimal PCE. Maximum PCE of over 2.3% were recorded for compounds **1** and **3**. This study showcased the potential of the anthanthrene scaffold as a versatile building block for organic electronics and the development of a second generation of small molecules specifically designed for OFETs and polymeric analogues for solar cells is under way.

Experimental

Transistor fabrication and characterization

Bottom-gate bottom-contact substrates were purchased from Fraunhofer IPMS (interdigitated S/D electrodes, width 10 000 μm and length 20 μm, $C_i \approx 14$ nF cm^{-2}) and were cleaned sequentially with acetone, IPA and water twice. For the formation of the ODTS-SAM the substrates were treated with O_2 plasma (5 minutes, 100 W) then placed on the spin-coater and 70 uL solution of octadecyltrimethoxysilane (3 mM in anh. chlorobenzene) was dropped on the substrates and after 10 seconds of self-organization spun at 1500 rpm. The substrates were then left overnight in a covered Petri dish with 30% aq. ammonia vapors. Finally the substrates were sonicated in toluene for 10 minutes and annealed at 110 °C for 5 minutes prior to the active layer deposition. The active layers were prepare by dispensing one drop of the semiconductor solution in chloroform (10 mg ml^{-1}) to the spinning substrate at 5000 rpm giving a uniform film of *ca.* 50 nm. In case of solvent annealing, the substrates were transferred to a covered Petri dish containing 1 ml of the appropriate solvent and left for 1 hour.

The field-effect transistors were characterized in a nitrogen-filled glovebox with an Agilent B1500A semiconductor parameter analyzer. The field-effect mobilities were calculated from the well-resolved saturation regions using the following equation:

$$I_{ds} = \frac{WC_i\mu}{2L}(V_{gs} - V_T)^2$$

Solar cells fabrication and characterization

Devices were fabricated in ambient conditions on indium tin oxide (ITO) coated glass substrates with a sheet resistance 15 Ω $square^{-1}$. The substrates were cleaned by sonication in acetone and isopropanol for 15 min each, blown dry with a nitrogen gun and treated with O_2 plasma. A 50 nm thick PEDOT:PSS layer (Clevios P4083, filtered 0.45 μm) was deposited *via* spin-coating followed by the deposition of the active layer from $CHCl_3$ solution (10 mg ml^{-1} concentration of donor with the appropriate concentration of $P_{61}CBM$ (purchased from SolenneBV)). The active layer solution was dispensed using a micropipette to the spinning substrate at 5000 rpm. For solvent annealing, the substrates were transferred to a covered Petri dish containing 1 ml of the appropriate solvent. After 15 minutes the substrates were blown dry and transferred to a nitrogen filled glovebox for electrode deposition. LiF (0.7 nm) and Al (100 nm) were thermally evaporated using a shadow mask with an active surface area of 10 mm^2. Thermal annealing in a nitrogen filled glovebox was performed on a hotplate (80 °C, 5 minutes) on the completed devices.

The solar cells were characterized in the dark and under illumination of a solar simulator (AM 1.5 Global spectrum with 100 mW cm^{-2} intensity). *I–V* characteristics were recorded using a Keithley 2400 source meter. All *I–V* measurements were carried out in a nitrogen filled glovebox. Layer thicknesses were measured with a Bruker Dektak stylus profilometer. External quantum efficiency (EQE) measurements were performed in a nitrogen-filled glovebox using a home-built setup including a monochromator, chopper, lock-in amplifier, xenon arc lamp and a reference Si photodiode.

Thin film absorption and AFM

The absorption spectra were recorded using an ultraviolet-visible spectrophotometer (Perkin-Elmer Lambda 1050) and the atomic force microscopy images were recorded in tapping mode (Dimension V SPM, Veeco). The film were deposited on a cleaned glass slide using the same spin-coating recipes as for the device fabrication and the annealing were performed in an identical fashion.

Acknowledgements

J.-B. G. thanks E. Glowacki, M. Scharber and P. Denk for helpful discussion and training, the National Sciences and Engineering Council of Canada (NSERC) for a Ph.D. scholarship, the Centre Québécois sur les Matériaux Fonctionnels (CQMF) and the Fond de Recherche du Québec – Nature et Technologies (FRQ-NT) for the funding that allowed a visit to LIOS where this work was performed.

Notes and references

1 Q. Ye and C. Chi, *Chem. Mater.*, 2014, **26**, 4046–4056.
2 W. Pisula, X. Feng and K. Müllen, *Adv. Mater.*, 2010, **22**, 3634–3649.
3 Y. Shu, G. E. Collis, C. J. Dunn, P. Kemppinen, K. N. Winzenberg, R. M. Williamson, A. Bilic, T. B. Singh, M. Bown and C. R. McNeill, *J. Mater. Chem. C*, 2013, **1**, 6299–6307.
4 S. Xiao, S. J. Kang, Y. Wu, S. Ahn, J. B. Kim, Y.-L. Loo, T. Siegrist, M. L. Steigerwald, H. Li and C. Nuckolls, *Chem. Sci.*, 2013, **4**, 2018–2023.
5 J. Mei, Y. Diao, A. L. Appleton, L. Fang and Z. Bao, *J. Am. Chem. Soc.*, 2013, **135**, 6724–6746.
6 J. Kwon, J.-P. Hong, W. Lee, S. Noh, C. Lee, S. Lee and J.-I. Hong, *Org. Electron.*, 2010, **11**, 1103–1110.
7 E. D. Glowacki, L. Leonat, G. Voss, M. Bodea, Z. Bozkurt, M. Irimia-Vladu, S. Bauer and N. S. Sariciftci, *Proc. SPIE*, 2011, **8118**, 81180M.
8 C. Wang, H. Dong, W. Hu, Y. Liu and D. Zhu, *Chem. Rev.*, 2012, **112**, 2208–2267.
9 L. Zhang, A. Fonari, Y. Liu, A.-L. M. Hoyt, H. Lee, D. Granger, S. Parkin, T. P. Russell, J. E. Anthony, J.-L. Brédas, V. Coropceanu and A. L. Briseno, *J. Am. Chem. Soc.*, 2014, **136**, 9248–9251.
10 E. Clar and R. Schoental, *Polycyclic hydrocarbons*, Academic Press, New York, 1964, vol. 2.
11 J. E. Anthony, *Chem. Rev.*, 2006, **106**, 5028–5048.
12 X. Zhan, A. Facchetti, S. Barlow, T. J. Marks, M. A. Ratner, M. R. Wasielewski and S. R. Marder, *Adv. Mater.*, 2011, **23**, 268–284.
13 H. Dong, X. Fu, J. Liu, Z. Wang and W. Hu, *Adv. Mater.*, 2013, **25**, 6158–9183.
14 J.-B. Giguére, J. Boismenu-Lavoie and J.-F. Morin, *J. Org. Chem.*, 2014, **79**, 2404–2418.
15 J.-B. Giguère and J.-F. Morin, *J. Org. Chem.*, 2013, **78**, 12769–12778.
16 J.-B. Giguère, Q. Verolet and J.-F. Morin, *Chem.–Eur. J.*, 2013, **19**, 372–381.
17 S. Hitosugi, H. Isobe, S. Kamata and T. Matsuno, *Chem. Sci.*, 2013, **4**, 3179–3183.
18 B. K. Shah, D. C. Neckers, J. Shi, E. W. Forsythe and D. Morton, *Chem. Mater.*, 2006, **18**, 603–608.
19 B. K. Shah, D. C. Neckers, J. Shi, E. W. Forsythe and D. Morton, *J. Phys. Chem.*, 2005, **109**, 7677–7681.
20 L. Zhang, B. Walker, F. Liu, N. S. Colella, S. C. Mannsfeld, J. J. Watkins, T.-Q. Nguyen and A. L. Briseno, *J. Mater. Chem.*, 2012, **22**, 4266–4268.
21 L. Zhang, A. Fonari, Y. Zhang, G. Zhao, V. Coropceanu, W. Hu, S. Parkin, J.-L. Brédas and A. L. Briseno, *Chem.–Eur. J.*, 2013, **19**, 17907–17916.
22 A. Broggi, I. Tomasi, L. Bianchi, A. Marrocchi and L. Vaccaro, *ChemPlusChem*, 2014, **79**, 486–507.
23 X. Sun, C. Di and Y. Liu, *J. Mater. Chem.*, 2010, **20**, 2599–2611.
24 D. D. C. Bradley, M. Heeney, N. Stingelin-Stutzmann, T. D. Anthopoulos, J. Smith, R. Hamilton and I. McCulloch, *J. Mater. Chem.*, 2010, **20**, 2562–2574.
25 Y. Li, C. Liu, A. Kumatani, P. Darmawan, T. Minari and K. Tsukagoshi, *Org. Electron.*, 2012, **13**, 264–272.
26 J. Shin, N. S. Kang, K. H. Kim, T. W. Lee, J.-I. Jin, M. Kim, K. Lee, B. K. Ju, J.-M. Hong and D. H. Choi, *Chem. Commun.*, 2012, **48**, 8490–8492.
27 Z. H. Kim, D. H. Choi, K. Lee, D. H. Lee, S. Y. Bae, M. J. Cho, K. H. Kim, C. E. Park, K. H. Jung and D. S. Chung, *Chem. Commun.*, 2009, 5290–5292.
28 F. Würthner, T. E. Kaiser and C. R. Saha-Möller, *Angew. Chem., Int. Ed.*, 2011, **50**, 3376–3410.
29 M. C. Scharber, D. Mühlbacher, M. Koppe, P. Denk, C. Waldauf, A. J. Heeger and C. J. Brabec, *Adv. Mater.*, 2006, **18**, 789–794.
30 J. Wang and B. Qi, *Phys. Chem. Chem. Phys.*, 2013, **15**, 8972–8982.